Mem. S.A.It. Vol. 81, 123

Memorie della

Multifrequency tests of dark matter sources

Aldo Morselli

INFN Roma Tor Vergata, e-mail: aldo.morselli@roma2.infn.it

Abstract. To uncover the dark matter, to connect what is astrophysically observed to what will be seen as new particles produced in the LHC, we need new measurements. The Fermi Large Area Telescope is providing the measurement of the high energy (20 GeV to 1 TeV) cosmic ray electrons and positrons spectrum with unprecedented accuracy. This measurement represents a unique probe for studying the origin and diffusive propagation of cosmic rays as well as for looking for possible evidences of Dark Matter. In this framework, we discuss possible interpretations of Fermi results in relation with other recent experimental data on energetic electrons and positrons and with recent results in the searches of gamma-ray fluxes coming from WIMP pair annihilations in the sky.

Key words. Dark Matter — Cosmic rays

1. Introduction

The PAMELA (a Payload for Antimatter Matter Exploration and Light-nuclei Astrophysics) experiment is a satellite-borne apparatus designed to study charged particles in the cosmic radiation with a particular focus on antiparticles (antiprotons and positrons) Picozza (2003). The PAMELA antiproton data Adriani (2000) are shown in figure 1 (left) together with the antiproton flux expected from standard secondary production. Cosmic ray propagation and production of secondary particles and isotopes is calculated using the GALPROP code Strong (2000). The lines show the minimal and maximal fluxes as calculated in models with different propagation parameters tuned to match the boron-to-carbon ratio in cosmic rays (Strong (2000), Moskalenko (2000), Lionetto (2000), Ptuskin (2000)). The antiproton data collected by PAMELA Adriani (2000) and BESS Abe (2000) are consistent with each other and with predictions for secondary antiproton flux thus excluding a strong antiproton signal from exotic processes. Figure 1 (right) is made in the framework of minimal supergravity (mSUGRA) by fixing the less sensitive parameters A_0, $\tan\beta$ and $\mathrm{sign}(\mu) = +1$ and in the case of a clumpiness factor 10 and $\tan(\beta) = 55$. Following the analysis in Lionetto (2000), the region below the line in figure 1 (right) can be excluded based on antiproton data.

This result can be compared with estimates based on Fermi five-years sensitivity to WIMP annihilation photons (continuum spectrum) from the Galactic center as shown in figure 2 (left) Morselli (2000); Cesarini (2000). The red band is the cosmologically allowed region by WMAP Spergel (2000); the region above the blue line ($M_{WIMP} \sim 200$ GeV) is not observable by Fermi due to the higher WIMP mass as one moves to higher $M_{1/2}$. The dark matter halo used for the Fermi indirect search sensitivity estimate is a truncated

Send offprint requests to: A. Morselli

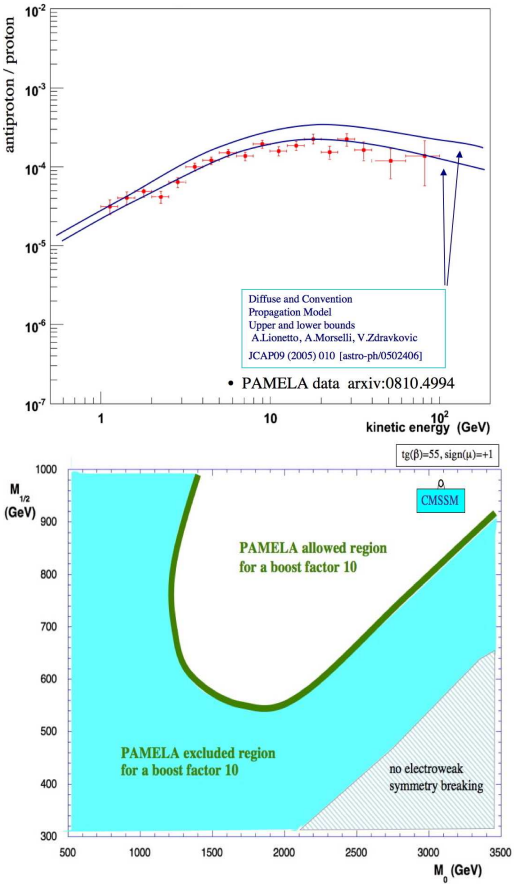

Fig. 1. *Left:* The antiproton-to-proton flux ratio as measured by PAMELA The lines show an approximate range expected for the standard secondary production. *Right:* PAMELA excluded region in a clumpy halo scenario for a boost factor 10 in the framework of minimal supergravity (mSUGRA) in the case of tan(β) = 55

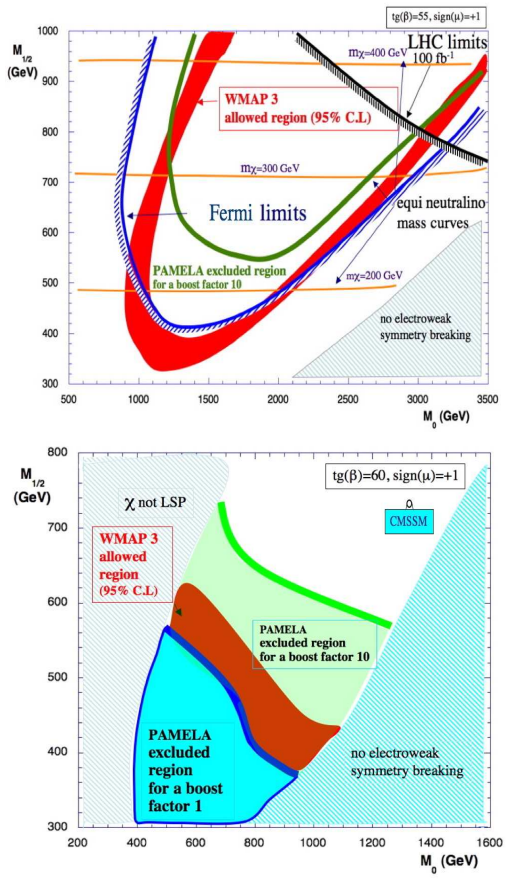

Fig. 2. *Left:* Sensitivity plot for observation of mSUGRA for PAMELA, LHC and Fermi for tan(β) = 55 (left) and for PAMELA and Fermi for tan(β) = 60 (right)

Navarro, Frank and White (NFW) halo profile. For steeper halo profiles (like the Moore profile) the Fermi limits move up, covering a wider WMAP allowed region, while for less steep profile (like the isothermal profile) the Fermi limits move down, covering less WMAP allowed region. The LHC accelerator limits are from Baer (2000).

Figure 2 (right) is the same of the figure on the left but for tan(β) = 60. It can be seen that for a clumpiness factor 10 all the WMAP region is already excluded. For larger value of tan(β) the excluded parameter space is even larger, while for lower values the capability of the antiprotons flux to probe the mSUGRA scenario is very weak (Lionetto (2000),Morselli (2000)).

2. Positron fraction and electron + positron flux

Contrary to the antiproton to proton ratio data, the PAMELA positron fraction data

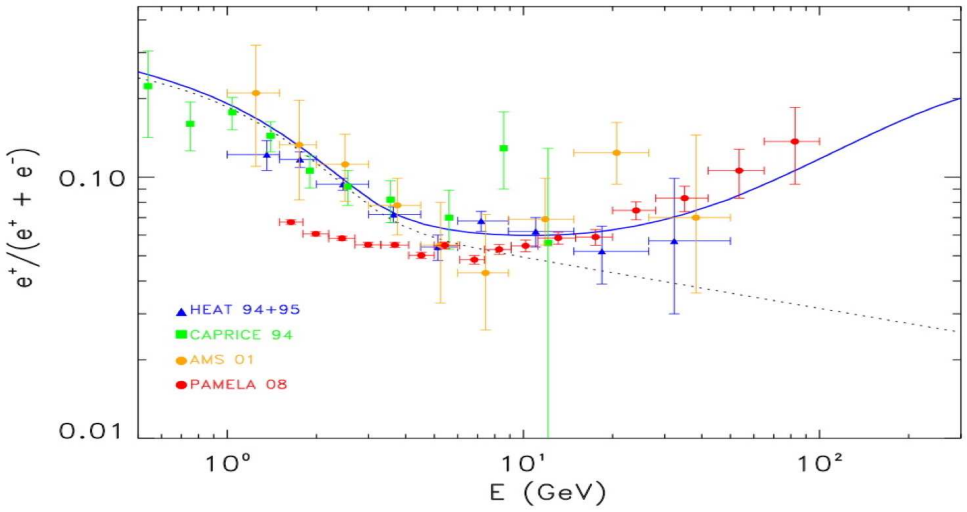

Fig. 3. PAMELA data and a possible contribution from Monogem and Geminga pulsars D.Grasso (2000). Black-dotted line shows the background from secondary positrons in cosmic rays from GALPROP

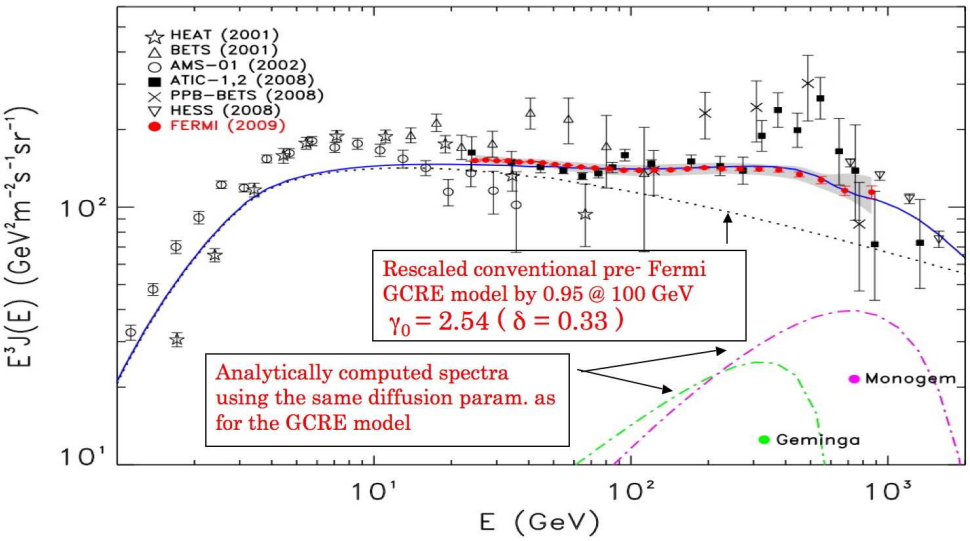

Fig. 4. Electron-plus-positron spectrum (blue continuos line) for the same scenario as in figure 3. The gray band represents systematic errors on the Fermi-LATdata Abdo (2000)

Adriani (2000) exhibit an excess above ~10 GeV that it is very difficult to explain with secondary production Strong (2000),Lionetto (2000) Morselli (2000). We note that the change in the positron fraction data below ~10 GeV is probably due to the solar modulation and change in the polarity of the solar magnetic field compared to the previous cycle. Recently the experimental information available on the Cosmic Ray Electron (CRE)

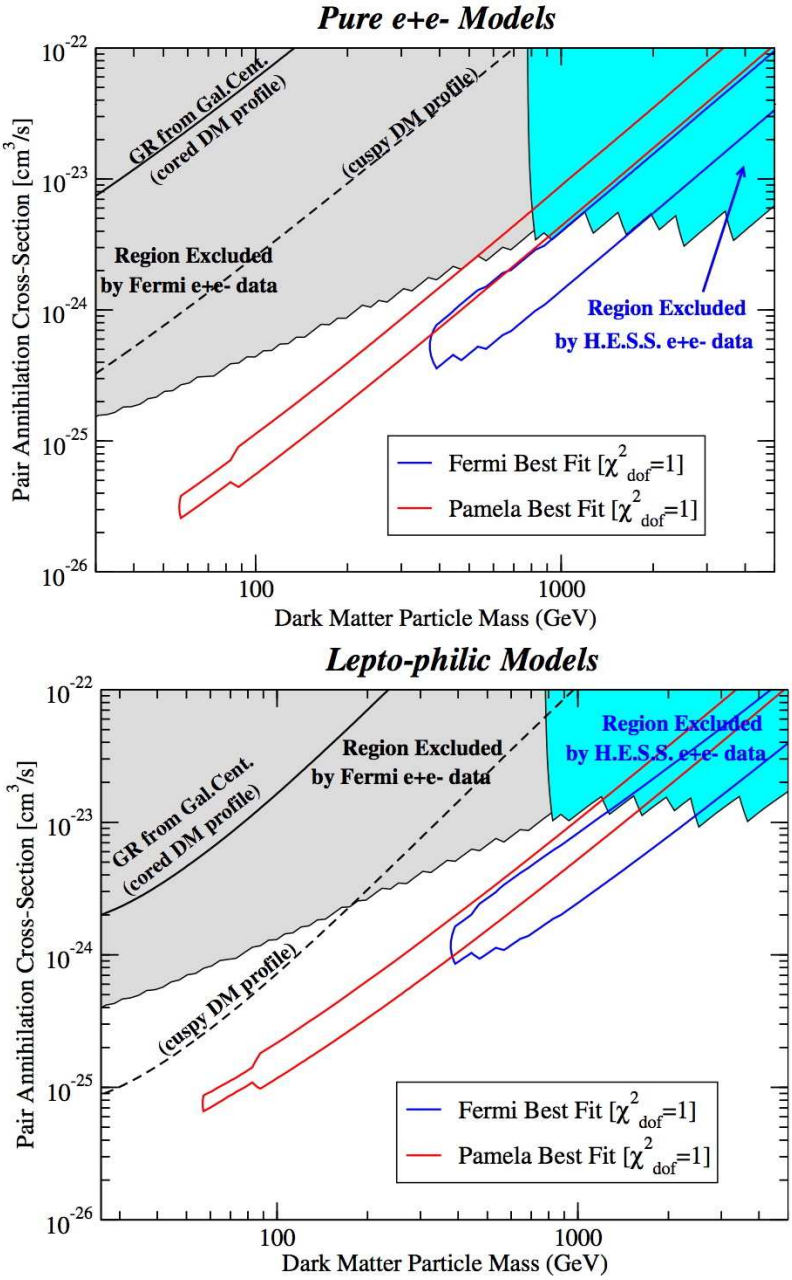

Fig. 5. The parameter space of particle dark matter mass versus pair-annihilation rate, for models where dark matter annihilates into monochromatic $e^{\pm}$ (up) and "lepto-philic" models (down) where the dark matter pair annihilates democratically into the three charged lepton species. Models inside the regions shaded in gray and cyan over-produce $e^{\pm}$ from dark matter annihilation with respect to the Fermi-LAT and H.E.S.S. measurements, at the 2-σ level. The red and blue contours outline the regions where the χ^2 per degree of freedom for fits to the PAMELA and Fermi-LAT data is at or below 1.

spectrum has been dramatically expanded as the Fermi-LAT Collaboration has reported a high precision measurement of the electron spectrum from 20 GeV to 1 TeV performed with its Large Area Telescope (LAT) Abdo (2000). The spectrum shows no prominent spectral features, and is significantly harder than that inferred from several previous experiments. The temptation to claim the discovery of dark matter is strong but there are competing astrophysical sources, such as pulsars, that can give strong flux of primary positrons and electrons (see Boulares (2000), Aharonian (2000), Coutu (2000), D.Grasso (2000) and references therein). At energies between 100 GeV and 1 TeV the electron flux reaching the Earth may be the sum of an almost homogeneous and isotropic component produced by Galactic supernova remnants and the local contribution of a few pulsars with the latter expected to contribute more and more significantly as the energy increases.

Two pulsars, Monogem, at a distance of d=290 pc and Geminga, at a distance of d=160 pc, can give a significant contribution to the high energy electron and positron flux reaching the Earth and with a set of reasonable parameters of the model of electron production we can have a nice fit of the PAMELA and Fermi data (see figures 3 and 4) , but it is true that we have a lot of freedom in the choice of these parameters because we still do not know much about these processes, so further study on high energy emission from pulsars are needed in order to confirm or reject the pulsar hypothesis.

Nevertheless a dark matter interpretation of the Fermi-LAT and of the PAMELA data is still an open possibility. In Figure 5 is shown the parameter space of particle dark matter mass versus pair-annihilation rate, for models where dark matter annihilates into monochromatic $e^{\pm}$ D.Grasso (2000). The preferred range for the dark matter mass lies between 400 GeV and 1-2 TeV, with larger masses increasingly constrained by the H.E.S.S. results. The required annihilation rates, when employing the dark matter density profile imply typical boost factors ranging between 20 and 100, when compared to the value $\langle\sigma v\rangle \sim 3 \times 10^{-26}$ cm^3/sec expected for a thermally produced dark matter particle relic.

How can one distinguish between the contributions of pulsars and dark matter annihilations? Most likely, a confirmation of the dark matter signal will require a consistency between different experiments and new measurements of the reported excesses with large statistics. The observed excess in the positron fraction should be consistent with corresponding signals in absolute positron and electron fluxes in the PAMELA data and all lepton data collected by Fermi Atwood (2000). Fermi has a large effective area and long projected lifetime, 5 years nominal with a goal 10 years mission, which makes it an excellent detector of cosmic-ray electrons up to ∼1 TeV. Future Fermi measurements of the total lepton flux with large statistics will be able to distinguish a gradual change in slope with a sharp cutoff with high confidence Baltz (2000). The latter, can be an indication in favor of the dark matter hypothesis. A strong leptonic signal should be accompanied by a boost in the γ-ray yield providing a distinct spectral signature detectable by Fermi.

The Galactic center (GC) is expected to be the strongest source of γ - rays from DM annihilation, due to its coincidence with the cusped part of the DM halo density prole

The flux depends from the WIMP mass $m_{\rm wimp}$, the total annihilation cross section times WIMP velocity σv and through the sum of all the photon yield dN_f/dE per each annihilation channel weighted by the corresponding branching ratio B_f. Apart from the $\tau\bar{\tau}$ channel, the photon yields are quite similar and depends from the neutralino mass. So fixing the halo density profile (for example a NFW profile), a dominant annihilation channel (that is $b\bar{b}$, $t\bar{t}$, W^+W^-, ...) and the corresponding yield, it is possible to perform a scan in the plane ($m_{\rm wimp}$, σv) in order to determine the GLAST reach and the regions that are already excluded by the EGRET data in the 2 degrees region around the galactic center Cesarini (2000), Mayer (2000), i.e. the flux predicted by the susy+background model must not exceed the total flux predicted from EGRET data. The result of the scan is given in figure 6 (left) for

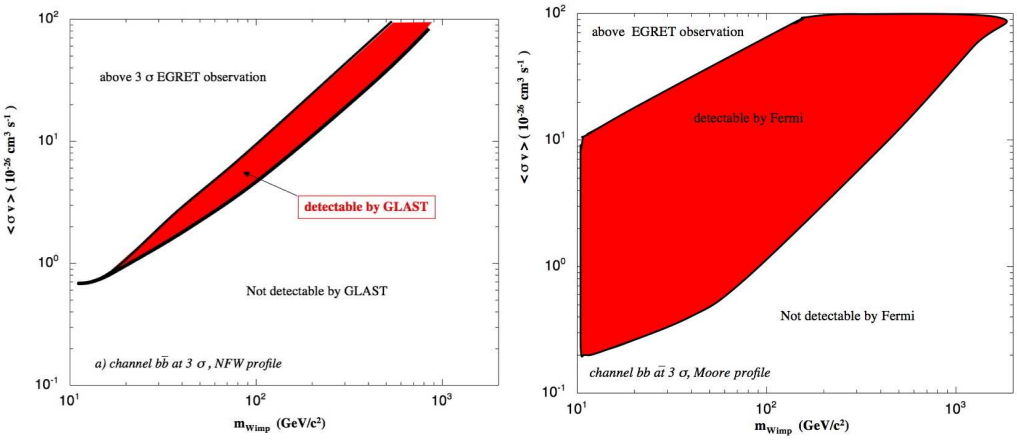

Fig. 6. *Left:* Cross Section times WIMP velocity versus the WIMP mass for the $b\bar{b}$ annihilation channel. The red region is allowed by EGRET data and detectable by GLAST for 3σ significance and 5 years of Fermi operation. *Right:* Same as figure on the left but for Sagittarius Dwarf assuming a Moore profile as described in Baltz (2000)

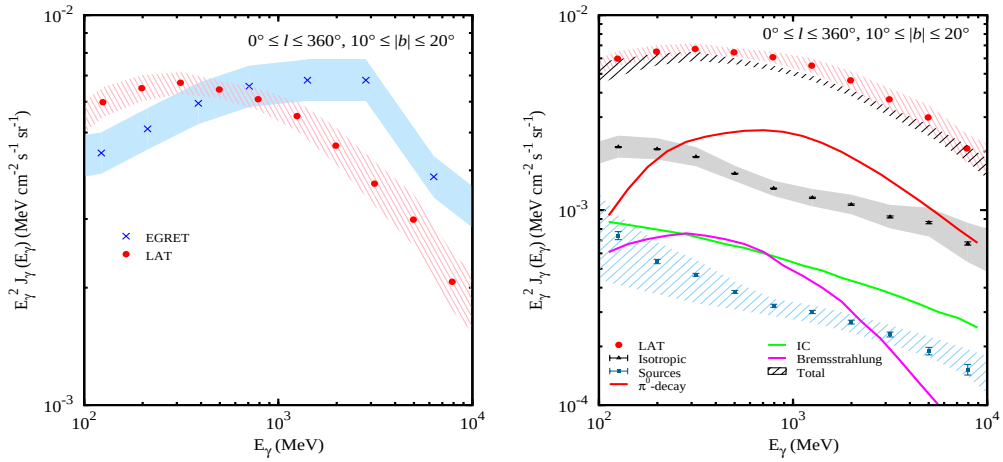

Fig. 7. *Left:* Preliminary diffuse emission intensity averaged over all Galactic longitudes for latitude range $10° \leq |b| \leq 20°$. Data points: Fermi LAT, red dots; EGRET, blue crosses. Systematic uncertainties: Fermi LAT, red; EGRET, blue. *Right:* Preliminary Fermi LAT data with model, source, and isotropic components for same sky region.

the Galactic center and in figure 6 (right) for Sagittarius Dwarf. For every couple of values ($m_{\rm wimp}$, σv) we compute the expected flux and we performed a standard χ^2 statistical analysis to see if GLAST is able to disentangle the WIMP contribution among the standard astrophysical π^0 background as used in Cesarini (2000). The result is given at a 3σ confidence level. The background uncertanties are reflected in the red regions. We assumed a total

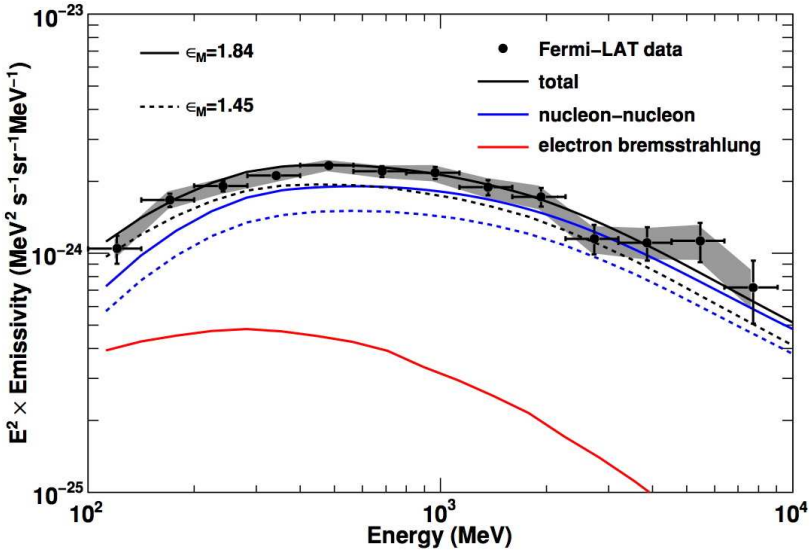

Fig. 8. Differential γ-ray emissivity from the local atomic hydrogen gas compared with the calculated γ-ray production. The horizontal and vertical error bars indicate the energy ranges and 1 σ statistical errors, respectively. Estimated systematic errors of the LAT data are indicated by the shaded area. A nucleus enhancement factor ϵ_M of 1.84 is assumed for the calculation of the γ-rays from nucleon-nucleon interactions. Dotted lines indicate the emissivities for the case of ϵ_M = 1.45, the lowest values in the referenced literature.

exposure of 3.7×10^{10} cm^2 s, for a period of 4 years of data taking and an angular resolution (at 10 GeV) of $\sim 3 \times 10^{-5}$ sr.

An excess in gamma-ray should also be seen in the Galactic diffuse spectrum. Figure 7 (left) shows the LAT data averaged over all Galactic longitudes and the latitude range $10^\circ \leq |b| \leq 20^\circ$. The hatched band surrounding the LAT data indicates the systematic uncertainty in the measurement due to the uncertainty in the effective area described above. Also shown on the right are the EGRET data for the same region of sky where one can see that the LAT-measured spectrum is significantly softer than the EGRET measurement Abdo (2000). Figure 7 (right) compares the LAT spectrum with the spectra of an *a priori* diffuse Galactic emission (DGE) model. While the LAT spectral shape is consistent with the DGE model used in this paper, the overall model emission is too low thus giving rise to a $\sim 10-15\%$ excess over the energy range 100 MeV to 10 GeV. However, the DGE model is based on pre Fermi data and knowledge of the DGE. The difference between the model and data is of the same order as the uncertainty in the measured CR nuclei spectra at the relevant energies. Overall, the agreement between the LAT-measured spectrum and the model shows that the fundamental processes are consistent with our data, thus providing a solid basis for future work understanding the DGE.

Also at higher latitudes for the moment we did no observed any excess. In figure 8 it is shown the diffuse γ-rays in a mid-latitude region in the third quadrant (Galactic longitude l from 200° to 260° and latitude $|b|$ from 22° to 60°). The region contains no known large molecular cloud and most of the atomic hydrogen is within 1 kpc of the solar system. The contributions of γ-ray point sources and inverse Compton scattering are estimated and subtracted. The residual γ-ray intensity exhibits a linear correlation with the atomic

gas column density in energy from 100 MeV to 10 GeV The differential emissivity from 100 MeV to 10 GeV agrees with calculations based on cosmic ray spectra consistent with those directly measured, at the 10 % level. The results obtained indicate that cosmic ray nuclei spectra within 1 kpc from the solar system in regions studied are close to the local interstellar spectra inferred from direct measurements at the Earth within ∼ 10 % Abdo (2000).

Finally a line at the WIMP mass, due to the 2γ production channel, could be observed as a feature in the astrophysical source spectrum Baltz (2000). Such an observation is a "smoking gun" for WIMP DM as it is difficult to explain by a process other than WIMP annihilation or decay and the presence of a feature due to annihilation into γZ in addition would be even more convincing.

3. Conclusion

Recent accurate measurements of cosmic-ray positrons and electrons by PAMELA, and Fermi have open a new era in particle astrophysics. The CRE spectrum measured by Fermi-LAT is significantly harder than previously thought on the basis of previous data. Adopting the presence of an extra $e^{\pm}$ primary component with ∼ 2.4 spectral index and $E_{cut} \sim 1TeV$ allow to consistently interpret Fermi-LAT CRE data (improving the fit), HESS and PAMELA. Such extra-component can be originated by pulsars for a reasonable choice of relevant parameters or by annihilating dark matter for model with $M_{DM} \sim 1TeV$. Improved analysis and complementary observations (CRE anisotropy, spectrum and angular distribution of diffuse γ, DM sources search in γ) are required to possibly discriminate the right scenario. Their exotic origin has to be confirmed by complimentary findings in γ-rays by Fermi and atmospheric Cherenkov telescopes, and by LHC in the debris of high-energy proton destructions. A positive answer will be a major breakthrough and will change our understanding of the universe forever. On the other hand, if it happens to be a conventional astrophysical source of cosmic rays, it will mean a direct detection of particles accelerated at an astronomical source, again a major breakthrough. In this case we will learn a whole lot about our local Galactic environment. However, independently on the origin of these excesses, exotic or conventional, we can expect very exciting several years ahead of us.

References

Abdo, A.A., et al. [Fermi Coll.], Physical Review Letters, 102, 181101 (2009) [arXiv:0905.0025]

Abdo, A.A., et al., [Fermi Coll.], ApJ 703 (2009) 1249-1256 [arXiv:0908.1171]

Abdo, A., et al. [Fermi Coll.], PRL submitted, Porter, T. A., et al. [Fermi Coll.], ICRC09 [arXiv:0907.0294]

Abe, K., et al. [BESS Coll.], arXiv:0805.1754

Adriani, O., et al.[PAMELA Coll.] Nature 458, 607, 2009 [arxiv:0810.4995]

Adriani, O., et al. [PAMELA Coll.] Phys. Rev. Lett. 102 (2009) 051101 [arxiv:0810.4994]

Aharonian, F. A., Atoyan, A. M., and Völk, H., J.,Astron. Astrophys. 294 (1995) L41

Atwood, W. B., et al., ApJ (2009) submitted

Baer, H., et al., JCAP 0408 (2004) 005

Baltz, E., et al., JCAP07 (2008) 013 [arXiv:0806.2911]

Boulares, A., APJ 342 (1989) 807-813

Cesarini, A., Fucito, F., Lionetto, A., Morselli, A., Ullio, P., Astropart. Phys. 21 (2004) 267

Coutu, S., et al., Astropart. Phys. 11 (1999) 429

Grasso, D., et al. Astroparticle Physics, accepted, [arXiv:0905.0636]

Lionetto, A., Morselli, A., and Zdravkovic, V. JCAP09 (2005) 010 [astro-ph/0502406]

Mayer-Hasselwander, H., et al., Astron. Astrophys. **335** (1998) 161.

Morselli, A., Moskalenko, I. PoS(idm2008)025 [arXiv:0811.3526]

Morselli, A., ICHEP 2006, Word Scientific (2007) 222-225, SBN-13 978-981-270-385-9

Morselli, A., at al., Nucl. Phys. 113B (2002) 213

Moskalenko, I. V., et al., ApJ 565 (2002) 280

Picozza, P., et al.[PAMELA Coll.], Astropart. Phys. 27 (2007) 296 [astro-ph/0608697]

Picozza, P. and Morselli, A., J. Phys. G: Nucl. Part. Phys. 29 (2003) 903 [astro-ph/0211286]
Picozza, P. and Morselli, A., World Scientific Publishing Co. [astro-ph/0604207]
Ptuskin, V. S., et al., ApJ 642 (2006) 902
Spergel, D. N., et al. [WMAP Coll.], ApJS 170 (2007) 377 [astro-ph/0603449]
Strong, A. W., Moskalenko, I. V., and Ptuskin, V. S., Annu. Rev. Nucl. Part. Sci. 57 (2007) 285
Strong, A. W. and Moskalenko, I. V., ApJ 509 (1998) 212, ApJ 493 (1998) 694